PNAS RESEARCH ARTICLE | MICROBIOLOGY OPEN ACCESS

Aerosolization of viable *Mycobacterium tuberculosis* bacilli by tuberculosis clinic attendees independent of sputum-Xpert Ultra status

Benjamin Patterson[a,1], Ryan Dinkele[b,c,1], Sophia Gessner[b,c], Anastasia Koch[b,c], Zeenat Hoosen[d], Vanessa January[d], Bryan Leonard[d], Andrea McKerry[d], Ronnett Seldon[d], Andiswa Vazi[d], Sabine Hermans[a], Frank Cobelens[a], Digby F. Warner[b,c,e,2], and Robin Wood[c,d,2]

Edited by Carl Nathan, Weill Medical College of Cornell University, New York, NY; received August 29, 2023; accepted February 1, 2024

Potential *Mycobacterium tuberculosis* (*Mtb*) transmission during different pulmonary tuberculosis (TB) disease states is poorly understood. We quantified viable aerosolized *Mtb* from TB clinic attendees following diagnosis and through six months' follow-up thereafter. Presumptive TB patients (n=102) were classified by laboratory, radiological, and clinical features into Group A: Sputum-Xpert Ultra-positive TB (n=52), Group B: Sputum-Xpert Ultra-negative TB (n=20), or Group C: TB undiagnosed (n=30). All groups were assessed for *Mtb* bioaerosol release at baseline, and subsequently at 2 wk, 2 mo, and 6 mo. Groups A and B were notified to the national TB program and received standard anti-TB chemotherapy; *Mtb* was isolated from 92% and 90% at presentation, 87% and 74% at 2 wk, 54% and 44% at 2 mo and 32% and 20% at 6 mo, respectively. Surprisingly, similar numbers were detected in Group C not initiating TB treatment: 93%, 70%, 48% and 22% at the same timepoints. A temporal association was observed between *Mtb* bioaerosol release and TB symptoms in all three groups. Persistence of *Mtb* bioaerosol positivity was observed in ~30% of participants irrespective of TB chemotherapy. Captured *Mtb* bacilli were predominantly acid-fast stain-negative and poorly culturable; however, three bioaerosol samples yielded sufficient biomass following culture for whole-genome sequencing, revealing two different *Mtb* lineages. Detection of viable aerosolized *Mtb* in clinic attendees, independent of TB diagnosis, suggests that unidentified *Mtb* transmitters might contribute a significant attributable proportion of community exposure. Additional longitudinal studies with sputum culture-positive and -negative control participants are required to investigate this possibility.

tuberculosis | aerosol sampling | subclinical

Significance

Knowing whether *Mycobacterium tuberculosis* (*Mtb*) bacilli are released in infectious aerosols throughout disease, treatment, and recovery phases is fundamental to understanding tuberculosis (TB) transmission. In this study, we used sensitive bioaerosol-capture technology to isolate viable *Mtb* bioaerosols in more than 90% of presumptive TB patients. Surprisingly, this percentage included individuals in whom pulmonary TB was not diagnosed. Over 6 mo follow-up of all participants, we observed a reduction in the proportion of *Mtb* bioaerosol-positivity independent of TB therapy. Moreover, viable *Mtb* organisms remained in approximately 30% of patients after treatment completion. Our results imply a complex *Mtb* host–pathogen interaction and provide insight into the difficulty of TB elimination in endemic areas despite effective chemotherapy of symptomatic TB cases.

Tuberculosis (TB) is uniquely characterized by obligate airborne transmission (1) with each new infection initiated following deposition of small diameter (<5 μm) *Mycobacterium tuberculosis* (*Mtb*)-containing bioaerosols in the distal lung of a susceptible human host (2). *Mtb* bioaerosols originate from infected individuals, and proximity to potential new hosts is generally necessary for rebreathing of viable organisms to occur—notable exceptions including environments in which individuals are confined with prolonged exposure to (re)circulating air (3). The onward propagation of *Mtb* therefore depends on the processes of natural production, expulsion, and survival of airborne bacilli in small aerosols. We recently reported considerable variability in cough-independent release of particulate matter—including *Mtb* organisms—among confirmed TB patients (4). However, the influence of TB disease stage on individual capacity for *Mtb* bioaerosol release is not known. Similarly, the speed and impact of standard TB chemotherapy on *Mtb* aerosolization has not been directly quantified.

The lung has been described as an aerosol generator (5): Every exhaled breath contains a small volume of peripheral lung fluid released by a fluid film burst mechanism in terminal bronchioles (6). Bioaerosol sampling captures this peripheral lung contribution and can be thought of as a noninvasive broncho-alveolar lavage. In contrast, sputum—which is produced in disease states—derives from mucin hyperproduction by goblet cells located in the upper conducting airways and confined to the trachea, bronchi, and larger bronchioles (7). Bioaerosols might, therefore, represent a more suitable sample to identify *Mtb* in the lung periphery and to investigate individuals with no or minimal sputum production, including subclinical TB disease (8). Notably, this sample has value both in demonstrating the presence of pathogen (*Mtb*) and, potentially, indicating a quantitative transmission risk.

Given the low airborne bacillary load, bioaerosol investigations depend on efficient capture and high-sensitivity detection of viable *Mtb* (9). Previous studies have

Author contributions: B.P., R.D., R.S., D.F.W., and R.W. designed research; R.D., S.G., A.K., Z.H., V.J., B.L., A.M., R.S., and A.V. performed research; R.D., S.G., A.K., Z.H., V.J., R.S., D.F.W., and R.W. contributed new reagents/analytic tools; B.P., R.D., A.K., S.H., F.C., D.F.W., and R.W. analyzed data; and B.P., R.D., S.G., A.K., S.H., F.C., D.F.W., and R.W. wrote the paper.

The authors declare no competing interest.

This article is a PNAS Direct Submission.

[1]B.P. and R.D. contributed equally to this work.

[2]To whom correspondence may be addressed. Email: digby.warner@uct.ac.za or robin.wood@hiv-research.org.za.

This article contains supporting information online at https://www.pnas.org/lookup/suppl/doi:10.1073/pnas.2314813121/-/DCSupplemental.

Published March 12, 2024.

explored respiratory maneuvers (10), collection devices (9), and the proximity of the participant to the collecting apparatus (11) to optimize capture of aerosolized *Mtb*. Groups employing cough aerosol (12) or facemask (13) sampling systems have achieved sensitivities of 30% and 91%, respectively, in sputum-positive patients. Combining advanced aerosol sampling and fluorescence detection systems, we have previously reported a 95% yield of viable *Mtb* in sputum-Xpert Ultra-positive individuals (14).

Utilizing the same technology, we aimed in the current study to investigate the capacity for viable *Mtb* release by TB clinic attendees categorized into three mutually exclusive groups based on South African National TB Program treatment and diagnostic protocols (15): laboratory-confirmed (sputum-Xpert Ultra-positive) TB (group A), sputum-Xpert Ultra-negative TB (group B), and those not diagnosed with TB (group C). By sampling all participants at defined intervals (approximately 2 wk, 2 mo, and 6 mo) after initial presentation, we further aimed to determine the impact of standard TB chemotherapy on *Mtb* bioaerosol production. The results presented here reveal the unexpected production of *Mtb* bioaerosols by non-TB patients, a time-dependent (not drug-dependent) decline in bioaerosol positivity, and the sustained detection of *Mtb* bioaerosols in a proportion of confirmed TB patients despite completion of the standard 6-mo combination regimen.

Results

Demographic and Symptomatic Characteristics of the Study Cohort. We recruited consecutive presumptive pulmonary TB patients over the age of 13 who self-presented to two community clinics serving two high-density, peri-urban residential areas southwest of Cape Town, South Africa. The final study population consisted of 102 TB clinic attendees (Table 1) who underwent repeated bioaerosol sampling between 15 May 2020 and 27 May 2022.

Of the participants sampled, 52 were sputum-Xpert Ultra-positive (group A); 20 were diagnosed as sputum-Xpert Ultra-negative TB (group B), 19 based on chest radiography and one on clinical suspicion alone; and 30 were sputum-Xpert Ultra-negative and not diagnosed with TB during 6 mo of follow-up visits (group C). One participant initially categorized as group C was reclassified to group B following radiographic TB diagnosis after the second (2-wk) visit. A greater proportion of sputum-Xpert Ultra-positivity than expected was thought to be related to the contemporaneous COVID-19 pandemic with individuals deferring initial visits to the clinic until symptoms were more significant or long-lasting. Eight participants in group C received short-course amoxicillin at initial presentation; no quinolones were prescribed. The remaining group C patients were not given a formal diagnosis. Patients were recruited from clinic X (n = 74) and clinic Y (n = 28); chi-squared testing found no difference in either

Table 1. Characteristics of patients stratified by each of the three diagnostic groups

Group*	A Sputum-Xpert Ultra-positive	B Sputum-Xpert Ultra-negative	C TB not diagnosed	*P*-value
n	52	20	30	
Age (mean (SD))	33.6 (9.8)	45.0 (10.9)	39.6 (11.7)	<0.001
Sex, male (%)	32 (61.5)	12 (60.0)	19 (63.3)	0.97
BMI (mean (SD))	19.9 (3.9)	20.6 (2.9)	23.9 (6.3)	0.003
HIV status (%)				0.018
Negative	33 (63.5)	5 (25.0)	18 (60.0)	
Positive	19 (36.5)	15 (75.0)	11 (36.7)	
Unknown	0 (0.0)	0 (0.0)	1 (3.3)	
On ARVs (%)				0.074
Nonadherent before the study	9 (50.0)	5 (35.7)	0 (0.0)	
No	4 (22.2)	3 (21.4)	3 (27.3)	
Yes	5 (27.8)	6 (42.9)	8 (72.7)	
CD4 count (median [IQR])	162 [95, 245]	144 [58, 214]	148 [86, 242]	0.684
On INH prophylaxis (%)				0.410
Nonadherent before the study	1 (2.2)	1 (5.3)	0 (0.0)	
No	43 (95.6)	18 (94.7)	21 (91.3)	
Yes	1 (2.2)	0 (0.0)	2 (8.7)	
Previous TB† (%)	17 (32.7)	13 (65.0)	15 (50.0)	0.035
No. of previous TB episodes (%)				0.401
1	11 (61.1)	8 (66.7)	13 (86.7)	
2	3 (16.7)	2 (16.7)	2 (13.3)	
3	4 (22.2)	2 (16.7)	0 (0.0)	
Preexisting lung disease (%)	3 (5.9)	0 (0.0)	4 (13.3)	0.195
Smoking (%)	25 (51.0)	10 (52.6)	10 (33.3)	0.250

Normally distributed continuous variables are reported as means with SD. For non-normally distributed variables, medians are reported with interquartile ranges [IQR]. Categorical variables are reported as counts with percentages in brackets. Normally distributed variables are compared using the Chi-squared test and non-normally distributed variables by Kruskal-Wallis Rank Sum test.

*BMI, body mass index; ARV, anti-retroviral; INH, isoniazid.

†For group A participants with a history of previous TB, 14/17 had at least a 2-y interval between previous TB treatment completion and recruitment into this study.

the proportions in each group ($P = 0.43$) or the rate of dropout at each visit ($P = 0.92$). Throughout the study, 16 participants were lost to follow-up, four relocated, four refused further sampling, three died, one was found to have multidrug-resistant TB and was excluded and one was censored. In total, there were 351 sampling visits with 73 (71.6%) participants completing all four visits: baseline, 2 wk, 2 mo, and 6 mo post initial presentation (*SI Appendix*, Fig. S1).

There were some differences in the baseline characteristics of the three groups (Table 1): Group A recorded the lowest median age and prevalence of previous TB, groups A and B had lower body mass indices than group C, and individuals in group B were older and had a higher prevalence of HIV infection. Notably, 45 participants (44.1%) had a history of previous TB.

At presentation (baseline sample), nearly all participants reported at least one symptom (Fig. 1*A*). The median number of symptoms was highest in group A (Fig. 1*B*), as expected; however, all three groups reported weight loss, persistent cough, loss of appetite, and night sweats as the most prevalent symptoms (Table 2).

Microbiological Detection of *Mtb* in Bioaerosol Samples. Each participant produced bioaerosols from three distinct respiratory maneuvers—forced vital capacity (FVC), tidal breathing, and voluntary cough. Putative 4-N, N-dimethylsamino-1,8-napthalimide-trehalose (DMN-trehalose)-positive *Mtb* bacilli with characteristic morphological appearance were detected for all three diagnostic groups. No significant differences were observed in the numbers of *Mtb* bacilli detected nor the prevalence of positive samples between the three respiratory maneuvers (*SI Appendix*, Fig. S2 *A* and *B*). Some individuals displayed a greater propensity for bacillary aerosolization in a single respiratory maneuver; however, this was not consistent for all participants tested (*SI Appendix*, Fig. S2*C*). Consequently, counts from respiratory maneuvers were pooled in subsequent analyses to compare participants in the three diagnostic categories, groups A–C.

Surprisingly, despite the differences reported in symptom number and severity, we observed no significant differences in median *Mtb* counts across groups A–C at baseline (Fig. 2*A*). Moreover, the prevalence of *Mtb*-containing bioaerosols was similar for all three groups (Fig. 2*B*), with *Mtb* detected in 92%, 90%, and 93% of bioaerosol samples in groups A, B, and C, respectively. There were no clinical or demographic variables predictive of a positive *Mtb* bioaerosol (Table 3).

Secular Trends in the Detection of *Mtb* in Bioaerosol Samples. In compliance with SA National TB Control Program policy, sputum-Xpert Ultra-positive (group A) and clinically diagnosed sputum-Xpert Ultra-negative (group B) TB patients were immediately started on 6 mo standard anti-TB therapy. Owing to the unexpectedly high baseline identification of aerosolized viable *Mtb* across all groups (A–C), we decided to monitor all participants for *Mtb* bioaerosol release and TB symptoms for 6 mo at defined intervals, regardless of clinical TB diagnosis. Therefore, serial bioaerosol sampling was conducted at approximately 2 wk (a 2-wk time point was targeted, but, in practice, the median was 19 d, IQR 10 d), 2 mo (median 61 d, IQR 19 d), and 6 mo (median 176 d, IQR 27 d) after initial enrollment (*SI Appendix*, Fig. S3).

Mtb bioaerosol numbers and the percentage of *Mtb*-positive bioaerosol samples decreased equivalently in all three groups over the 6 mo, irrespective of TB therapy (Fig. 3*A*), and there were no notable differences in the numeric trends between any of the three groups (Fig. 3*B*).

In groups A and B—comprising notified TB cases—*Mtb* was isolated in bioaerosol samples from 87% and 74% of participants at 2 wk, 54% and 44% at 2 mo, and 32% and 20% at 6 mo, respectively, with similar numbers detected for group C (70%, 48%, and 22%, respectively, at the same time points). Notably, the decline in bioaerosol positivity corresponded to a reduction in each TB symptom (persistent cough, fever, weight loss, and night sweats) for all three groups (Fig. 4).

The (*SI Appendix*, Fig. S4). The median time to clearance of *Mtb* bacilli from bioaerosol samples was 83 d (95% CI, 63 to 167 d) (Fig. 5*A*); stratification by treatment (Fig. 5*B*), previous history of TB (Fig. 5*C*), or HIV status (Fig. 5*D*) did not significantly alter the time to clearance (log-rank *P*-values 0.720, 0.687, and 0.399, respectively). The time to *Mtb* bacillary clearance was also not significantly different between patients recruited from clinic X and clinic Y. The median time to TB symptom resolution was 57 d (95% CI, 55 to 67 d) (Fig. 6*A*). There was no impact of treatment (Fig. 6*B*), a previous history of TB (Fig. 6*C*), or HIV status (Fig. 6*D*) on rate of symptom resolution (log-rank *P*-values, 0.223, 0.355, and 0.157, respectively).

To evaluate the possibility of a degradation in the reagents of the DMN-trehalose assay reducing sensitivity over time, DMN-trehalose *Mtb* bacilli counts were assessed for correlation with calendar date.

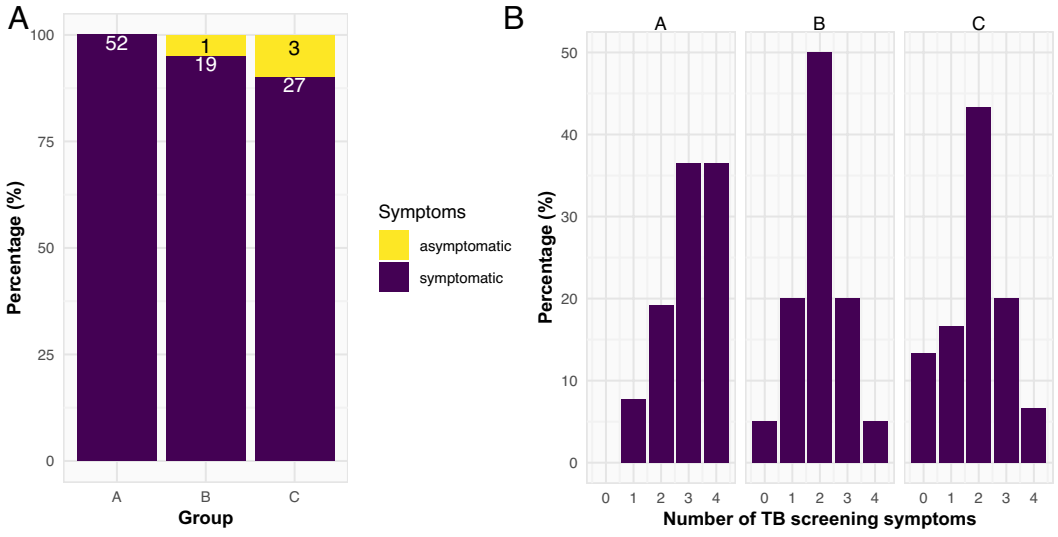

Fig. 1. Presentation of symptoms at baseline. (*A*) Percentage of participants with one or more self-reported symptoms. (*B*) Distribution of the number of symptoms per individual by diagnostic group; the median symptom number for groups A, B, and C was 3, 2, and 2, respectively.

Table 2. The prevalence of each of the symptoms identified by patient questionnaire at the initial visit stratified by diagnostic group

Group	A Sputum-Xpert Ultra-positive	B Sputum-Xpert Ultra-negative	C TB not diagnosed	*P*-value
n	52	20	30	
Persistent cough (%)	45 (86.5)	12 (60.0)	19 (63.3)	0.017
Weight loss (%)	46 (88.5)	16 (80.0)	20 (66.7)	0.057
Night sweats (%)	38 (73.1)	8 (40.0)	12 (40.0)	0.003
Loss of appetite (%)	28 (53.8)	4 (20.0)	6 (20.0)	0.002
Fever (%)	7 (13.5)	1 (5.0)	8 (26.7)	0.097
Hemoptysis (%)	5 (9.6)	0 (0.0)	2 (6.7)	0.508
Myalgias (%)	8 (15.4)	1 (5.0)	4 (13.3)	0.493
Anosmia (%)	1 (1.9)	1 (5.0)	0 (0.0)	0.440

To remove any effect of time since enrollment and treatment, the DMN-trehalose counts were separated into group and visit combinations; thus, any impact of the age of DMN-trehalose reagents could be isolated. The proportion of the variation explained by time was a median of 3% (R-squared range: <0.01 to 0.15).

Microscopic Characterization of *Mtb* Bacilli From Bioaerosol Samples. Mycobacteria, including *Mtb*, demonstrate morphological and metabolic plasticity in response to environmental and antibiotic stresses (16–18). We reasoned that if *Mtb* bacilli were exposed to antibiotics before aerosolization, a discernible change in bacterial morphology and/or metabolic state might be detectable between treatment groups. An important consideration before performing this analysis, however, was the previous observation that *Mtb* morphology, specifically cell length, can differ according to anatomical origin (19). To allow for data pooling, we first needed to confirm that the three maneuvers employed in this study produced *Mtb* from the same respiratory compartment. To this end, we compared the length distributions of *Mtb* detected from each respiratory maneuver at baseline (*SI Appendix*, Fig. S5). No significant differences were evident, suggesting that all bacilli were aerosolized from the peripheral lung by a conserved mechanism (4, 10).

As observed previously (20), we identified multiple DMN-trehalose staining profiles in *Mtb* bacilli captured from participant bioaerosols (*SI Appendix*, Fig. S6 *A* and *B*), with most baseline samples characterized by two or more distinct staining patterns (*SI Appendix*, Fig. S6*C*). For further microscopic analyses, the 6-mo sample was excluded as too few bacilli were detected to make reliable conclusions.

Polarity index, a metric summarizing the staining profile of synthetic trehalose probes along the medial axis, has previously been shown to differ significantly upon exposure to antibiotics (21). Comparing the average polarity index of bacilli from treated and untreated samples did not reveal significant differences at baseline or 2 wk. However, the polarity index of *Mtb* from treated individuals was slightly higher at 2 mo (Fig. 7*A*) and corresponded to a minor increase in cell length observed in the same samples (Fig. 7*B*). Despite these very slight changes in cell length and DMN-trehalose staining, no significant differences in clustering were observed between participants (*SI Appendix*, Fig. S7), suggesting that the treatment effect on bacterial phenotype was minor.

Genotypic and Genomic Confirmation of *Mtb* in Bioaerosol Samples. The apparent lack of a treatment effect on *Mtb* bioaerosol clearance was a surprising observation. To increase our confidence

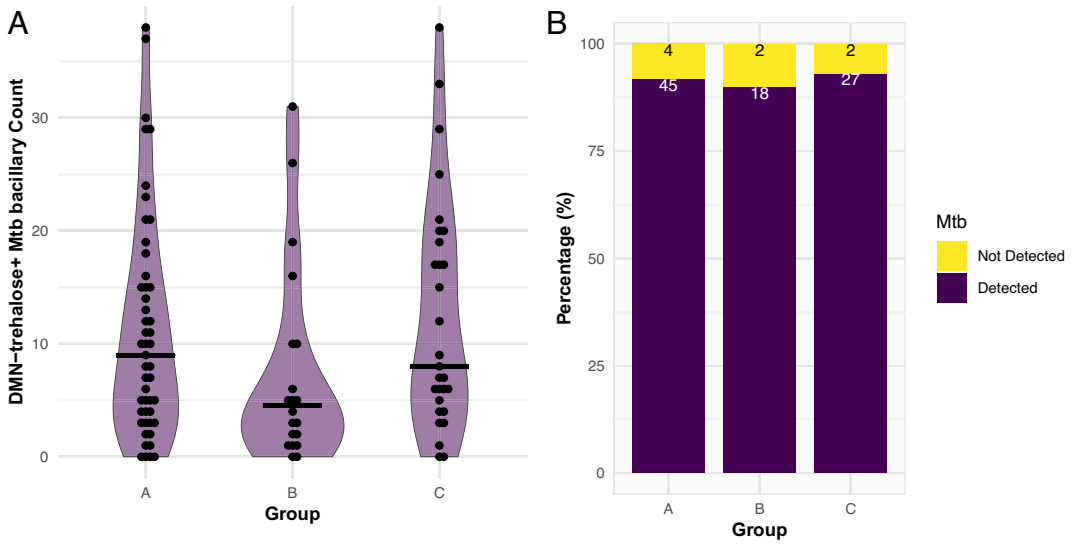

Fig. 2. The detection of *Mtb* bacilli in bioaerosol samples from all three diagnostic groups at baseline. (*A*) Counts of putative *Mtb* with medians 9, 4.5, and 8 (represented by the thick black bars) for groups A, B, and C, respectively. No difference was found between the groups with Wilcoxon rank-sum testing after Bonferroni correction for multiple comparisons. (*B*) Percentage *Mtb* bioaerosol positive samples per diagnostic group. Owing to contamination of the slides, four samples were uninterpretable; these are not included in the denominator of the prevalence proportions.

Table 3. Odds ratios for baseline demographic and clinical variables associated with baseline DMN-trehalose *Mtb* bacillary positivity

	Unadjusted odds ratio	CI low (2.5)	CI high (97.5)	*P*-value
Age				
<30	Reference			
≥30	1.84	0.26	10.37	0.443
Sex				
Male	Reference			
Female	1.81	0.3	19.33	0.514
Body mass index				
<20	Reference			
≥20	0.15	0	1.24	0.053
HIV status				
Negative	Reference			
Positive	0.82	0.14	4.69	0.792
Xpert Ultra				
Negative	Reference			
Positive	1	0.17	5.72	>0.99
Isoniazid preventive therapy*				
No	Reference			
Yes	0.28	0.03	15.2	0.765
Previous TB				
No	Reference			
Yes	1.45	0.26	9.91	0.647
Smoking history				
No	Reference			
Yes	1.55	0.28	10.59	0.589
Underlying lung disease*				
No	Reference			
Yes	0.69	0.08	30.22	0.529

*Haldane–Anscombe correction used for small samples.

in the *Mtb* assignments based on DMN-trehalose fluorescence, a second bioaerosol sample was collected in parallel from a subset of participants. The presence of *Mtb* bacilli in these samples was assessed using either conventional Auramine O (n = 44) and Ziehl–Neelsen (n = 50) staining or by means of a droplet digital (dd)PCR-based molecular assay targeting the *Mtb*-specific RD9 locus (n = 37), as reported previously (7). Sequentially selected samples included both baseline and subsequent visits. All (37/37) of the samples investigated by ddPCR were RD9 positive, confirming the presence of *Mtb* genomes (*SI Appendix*, Table S1 and Fig. S8). In contrast, Auramine O staining was positive in 82% (36/44) of samples, while Ziehl–Neelsen acid-fast staining was negative for all samples assayed.

Attempts to culture *Mtb* organisms from bioaerosol samples proved mostly unsuccessful despite extending the incubation period to 50 d in liquid medium. Five samples which exhibited growth were selected for whole-genome sequencing to ascertain the feasibility of detecting "transmitted" *Mtb* lineages using this approach (Table 4): two from sputum-Xpert Ultra-positive (group A) participants, one baseline and one at 6 mo, and three from sputum-Xpert Ultra-negative (group C) participants, two at baseline and one at 2 mo. Of these, only three samples provided data of sufficient quality to detect lineage-defining single nucleotide polymorphisms (SNPs) (22). On analysis, we determined that one sputum-Xpert Ultra-positive sample (group A, baseline) and one sputum-Xpert Ultra-negative sample (group C, baseline) belonged to lineage 4.9, with the third sample (group C, baseline) belonging to lineage 4.3 (Table 4). Analysis of all five samples using Kraken2 (23) revealed that reads mapping to the *Mtb* Complex (MTBC) were present in all samples, albeit at different proportions. In samples for which whole genome sequencing (WGS) data produced >30-fold coverage of the *Mtb* genome, almost all reads mapped to MTBC genomes present in the Kraken database. A significant proportion of reads in samples with lower coverage were reported as unclassified via the Kraken2 analysis, with 0.01 to 0.05% of reads mapping to *Mtb* (*SI Appendix*, Fig. S9). Other bacterial species identified in the samples by Kraken2 included *Samonella enterica* and *Brevibacterium lutoleum*.

Discussion

Current approaches to TB control are predicated on tenets which are increasingly being questioned as improved technologies enable insights into mycobacterial pathogenicity and the TB disease cycle that were previously inaccessible to investigation (24, 25). Among these are the reliance on sputum *Mtb* positivity as a marker of patient infectiousness (26), and the dependence on coughing as sole vehicle for aerosol *Mtb* release (4, 10, 14). Historically, these assumptions have constrained most TB transmission research to the identification and recruitment of sputum-Xpert Ultra-positive or sputum-smear-positive TB patients, even in those utilizing innovative approaches to identify the "missing" TB cases, such as

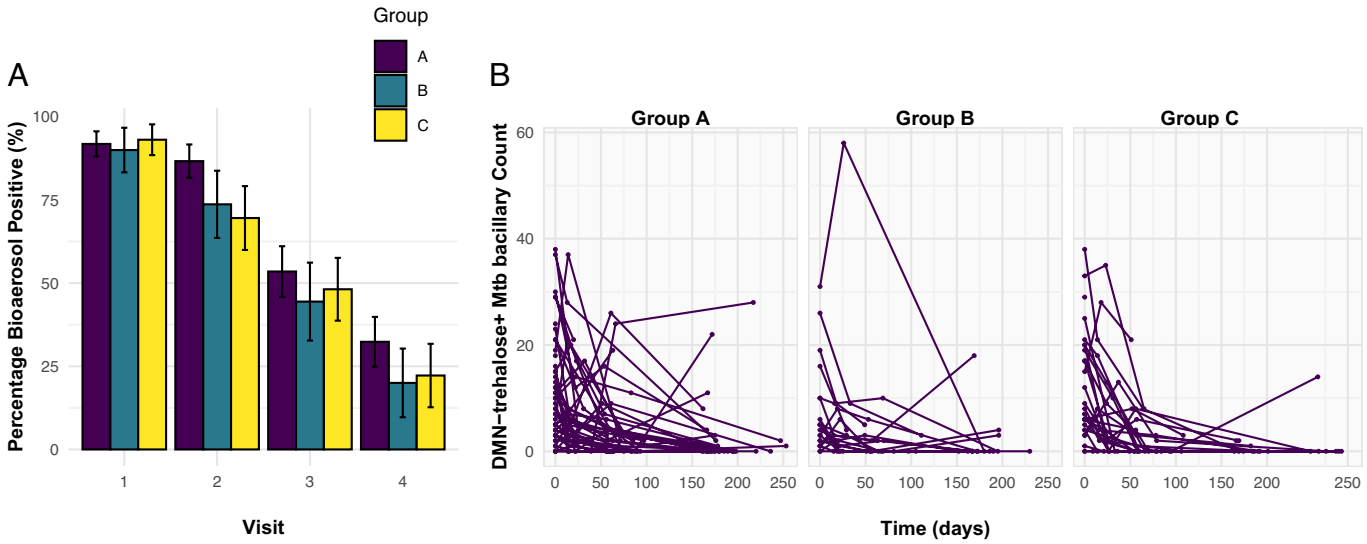

Fig. 3. The detection of *Mtb* bioaerosols decreased similarly in all three groups over 6 mo. (*A*) The percentage of bioaerosol samples that were positive for *Mtb*. The det.nominator is all visits yielding an interpretable sample. Thirteen samples were uninterpretable; these are not included in the denominator of the prevalence proportions. The error bars represent the SEM. Fisher's exact tests performed on each visit found no significant differences. (*B*) Secular trends in the number of *Mtb* detected in bioaerosol samples of each diagnostic group. Lines connect the samples from the same participant at each successive visit.

household contact investigations, and cough (12) or face-mask (13) sampling studies.

We previously reported the combined use of the RASC (respiratory aerosol sampling chamber), DMN-trehalose labeling, and fluorescence microscopy to identify viable aerosolized *Mtb* in most sputum-positive TB patients (11, 14, 27). The DMN-trehalose probe is incorporated into the mycobacterial cell wall by the antigen-85 mycolyl transferase complex (28); detection of a fluorescent DMN-trehalose signal in a whole mycobacterial cell therefore indicates a metabolically active organism (29).

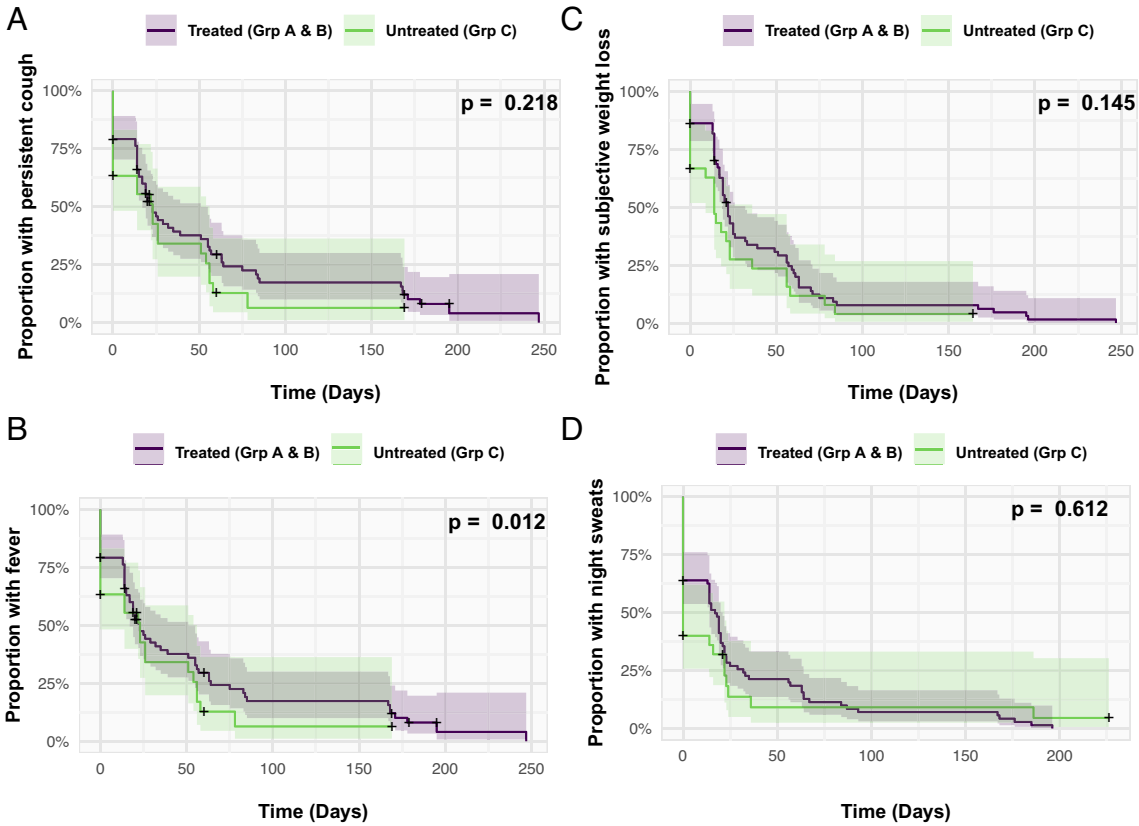

Fig. 4. Kaplan–Meier plots showing proportion with symptom resolution over time. The first visit at which each symptom is not reported is considered the time to resolution. Individuals reporting symptoms at the final visit are censored at the time of this visit. (*A*) shows the time to resolution of self-reported persistent cough, (*B*) fever, (*C*) subjective weight loss, and (*D*) night sweats. All plots compare TB patients on treatment (groups A and B) and those individuals not diagnosed with TB and therefore not treated (group C). If a symptom recurred after resolution, this was not included. The shaded areas represent 95% CI. Log-rank test *P*-values are given in the *Top Right* corner.

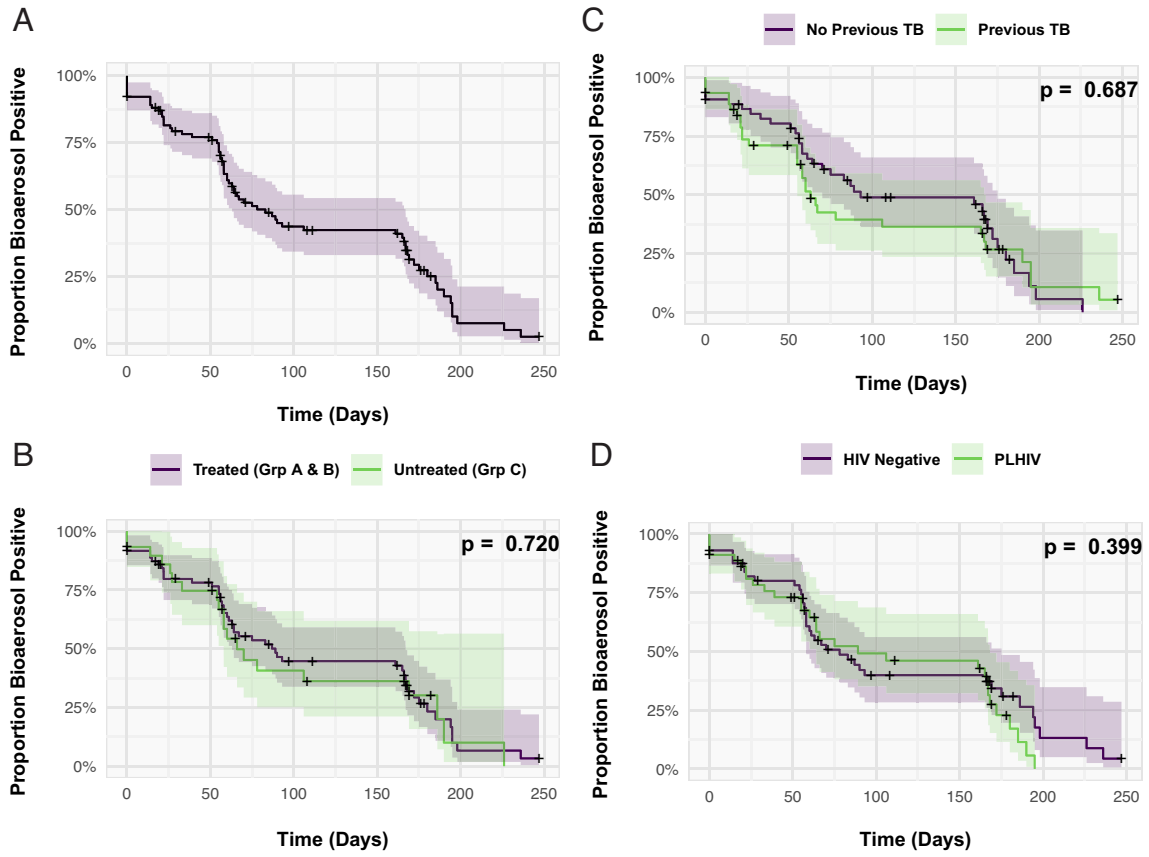

Fig. 5. Kaplan–Meier plots showing time to *Mtb* bacillary clearance from collected bioaerosol. The first visit at which *Mtb* is not detected in the sample is considered the time to clearance. Individuals with detectable *Mtb* at the final visit are censored at the time of this visit. (*A*) All participants. (*B*) TB patients on treatment (groups A and B) are separated from those individuals not diagnosed with TB and therefore not treated (group C). (*C*) Comparison of time to clearance between those with a previous history of TB and those without. (*D*) Participants separated according to HIV status. The shaded areas represent 95% CI. Log-rank test *P*-values are given in the *Top Right* corner for panels *B*–*D*. PLHIV, person living with HIV.

Prior studies of bacillary size, morphology, and staining characteristics have shown good agreement between patient samples and cultures of the laboratory strain, *Mtb* H37Rv (20). DMN-trehalose staining has also demonstrated characteristic bacillary morphological and staining phenotypes that reliably distinguish *Mtb* from non-mycobacteria (20). Given that most infections cannot be linked to an index case (30), we hypothesized that *Mtb* might be aerosolized by some sputum-Xpert Ultra-negative individuals who would, by definition, be excluded from conventional TB transmission studies. Therefore, the primary aim of the current work was to determine the capacity for bioaerosol *Mtb* release by sputum-Xpert Ultra-negative TB patients (group B) diagnosed on clinical presentation. By sampling all participants at defined intervals thereafter, we also aimed to ascertain the impact of standard TB chemotherapy on *Mtb* bioaerosol production.

We report two striking observations. First, we identified aerosolized *Mtb* in a large majority of both confirmed TB patients (sputum-Xpert Ultra-positive [group A] and sputum-Xpert Ultra-negative [group B]) and individuals excluded from a TB diagnosis (group C) at the initial clinic visit. In compliance with South African National TB Control Program policy, sputum-positive and clinically diagnosed sputum-negative TB patients immediately commenced 6 mo standard anti-TB therapy. And, owing to the high baseline identification of aerosolized viable *Mtb*, we monitored all participants—regardless of clinical TB diagnosis—for aerosolized *Mtb* and TB symptoms at defined intervals for 6 mo. This enabled the second major observation, namely that *Mtb* bioaerosol numbers and proportion positivity declined at similar rates irrespective of TB therapy. Notably, around 20% of all participants were aerosol positive at the final, 6-mo time point, albeit with very low *Mtb* bacillary numbers.

The unexpected detection of *Mtb* in bioaerosols from individuals without proven TB challenged us to confirm the *Mtb* assignation utilizing alternative (DMN-trehalose-independent) approaches, and to better define the phenotypes of bioaerosol *Mtb*. To further address specificity, a series of secondary aerosol samples collected at the same visit was analyzed by ddPCR targeting the RD9 locus, an *Mtb*-specific genetic marker (31); all samples were RD9 positive, confirming the presence of *Mtb* genomic DNA. A large proportion of aerosol samples were also positive under Auramine O staining, which is routinely applied for sputum-based *Mtb* identification, but they were acid-fast stain-negative using the Ziehl–Neelsen protocol. The superior sensitivity and specificity of Auramine O over Ziehl–Neelsen staining has been reported previously (32) and has been ascribed to the retention of Auramine O by the mycolic acid component of the mycobacterial cell wall (33)—a conclusion which supports the correlation between Auramine O and DMN-trehalose positivity. Notably, loss of acid-fastness occurs naturally in human TB disease and animal infection models (34), and has been attributed to changes in cell wall composition and/or architecture as a function of metabolic alterations during host colonization (33). Whether aerosol bacilli are specifically adapted to external passage and survival is uncertain; however, the complete absence of acid-fast organisms in these samples raises important

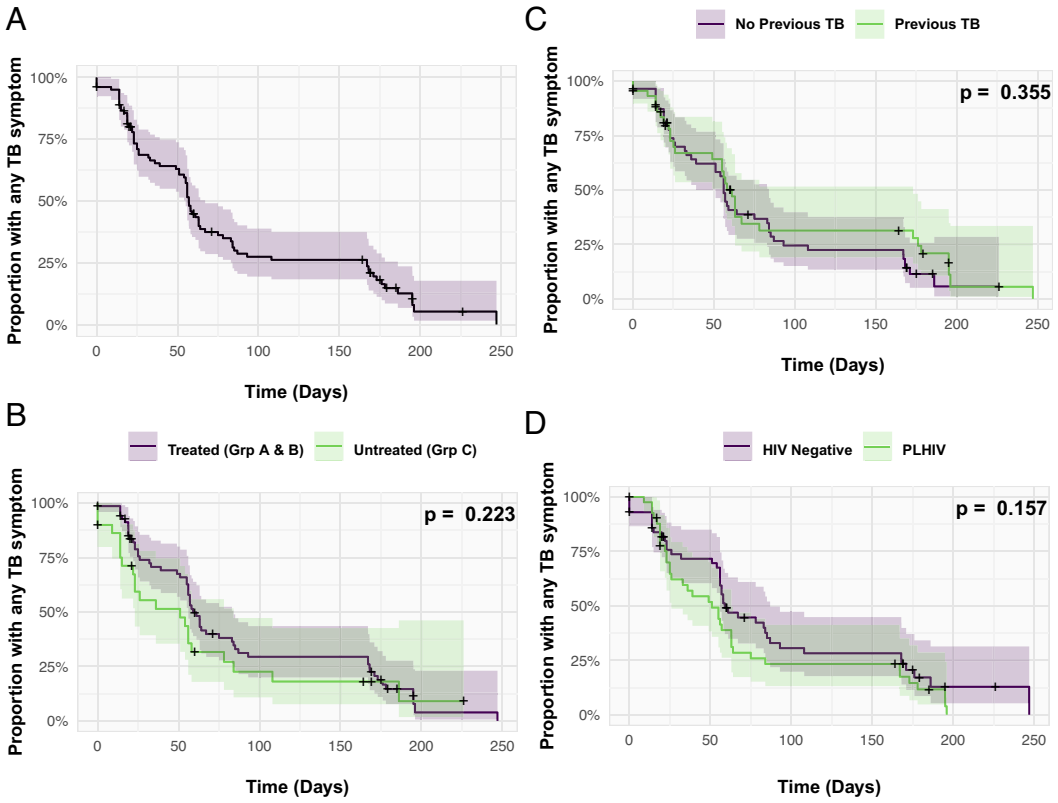

Fig. 6. Kaplan–Meier plots showing the proportion of individuals with any TB symptom (persistent cough, fever, weight loss, and night sweats) against days since first sampling. The first visit without reported symptoms is considered the time to clearance. Participants with symptoms at the final visit are censored at the time of this visit. (*A*) All participants. (*B*) Participants separated into TB patients on treatment (groups A and B) and those not diagnosed with TB and therefore not treated (group C). (*C*) Comparison of participants with a previous history of TB and without. (*D*) Comparison of participants according to HIV status. The shaded areas represent 95% CI. Log-rank test *P*-values are given in the *Top Right* corner for panels *B*–*D*. PLHIV, person living with HIV.

questions about the physiological state(s) of transmitted *Mtb* organisms.

Five samples that had been cultured for 50-d in 7H9 OADC media were selected for analysis via WGS to determine whether WGS could further validate the detection of genomes in bioaerosol samples, and more, if WGS data could provide information about the *Mtb* lineages observed. Three samples provided WGS data for which lineage associated SNPs could be reliably detected (Table 4). Two samples were classified as belonging to lineage 4.9 and one to lineage 4.3. Analysis of the data using Kraken2, a tool that assigns taxonomic labels to all sequencing reads in a sample (23), revealed that *Mtb* sequencing reads were present in all samples, albeit at different proportions. Notably, these analyses returned no evidence of reads mapping to NTMs, suggesting that NTMs were not a confounding presence in the microbiological (DMN-tre) or the genomic assays. In samples characterized by lower *Mtb* coverage and lower percentage reads mapping to the MTBC, a large proportion of reads were unclassified via Kraken2, highlighting the technical complexities of generating and analyzing WGS data from paucibacillary samples.

Importantly, the samples that provided reliable WGS data yielded >1,000 DNA copies as estimated by RD9 ddPCR. These data indicate that while WGS is feasible on bioaerosols, sufficient DNA is required to generate data of high enough quality to identify specific *Mtb* lineages. Future work to facilitate WGS of a broader number of samples could include optimization of DNA extraction techniques, culture, and possibly *Mtb* DNA enrichment prior to WGS (35–37).

A phenotype of poorly replicating, non-acid-fast *Mtb* able to cause TB in animal models with reversion to acid-fast staining was first identified from TB patients in 1883 (38). Subsequently isoniazid inhibition of mycolic acid biosynthesis demonstrated that cell wall organizational changes can be responsible for loss of acid-fast staining (39) and actively replicating acid-fast *Mtb* have been shown to convert to poorly replicating *Mtb* with an associated loss of acid-fast staining (33). The aerosol *Mtb* samples were poorly culturable, with only four of 64 (6.25%) yielding >1,000 DNA copies after 50 d liquid culture. Poor culturability is a well-known characteristic of *Mtb* derived from clinical specimens (40) with at least one prior study reporting that in 20 out of 25 sputum smear-positive samples >80% of the *Mtb* bacilli in the sample could only be detected after supplementation with resuscitation-promoting factor (41). Very recent work involving single-cell analyses of *Mtb* organisms in microfluidic devices has also utilized spent culture medium to ensure reproducible growth (42), suggesting that future bioaerosol studies should incorporate this approach.

The finding of *Mtb* bacilli by noninvasive sampling of pulmonary lining fluid (PLF) from the lung periphery is compatible with the high diagnostic yield of bronchoalveolar lavage (BAL) in sputum-negative TB (43) and consistent with previous evidence of transmission from this subgroup (44, 45). The identification of viable *Mtb* in a subset of TB patients at end-of-treatment (EOT) echoes previous findings of an 18F-fluorodeoxyglucose Positron Emission Tomography and Computerized Tomography (FDG-PET/CT) imaging study that tracked 99 HIV-negative patients through TB treatment and reported a range of outcomes with a proportion showing new FDG-avid lesions and ongoing inflammation (46). In that work, *Mtb* mRNA transcripts were found in 37% of sputum and 100% of BAL samples from EOT patients, implying the presence of live organisms. A further study of nonsterilizing cure found differentially culturable *Mtb* organisms in

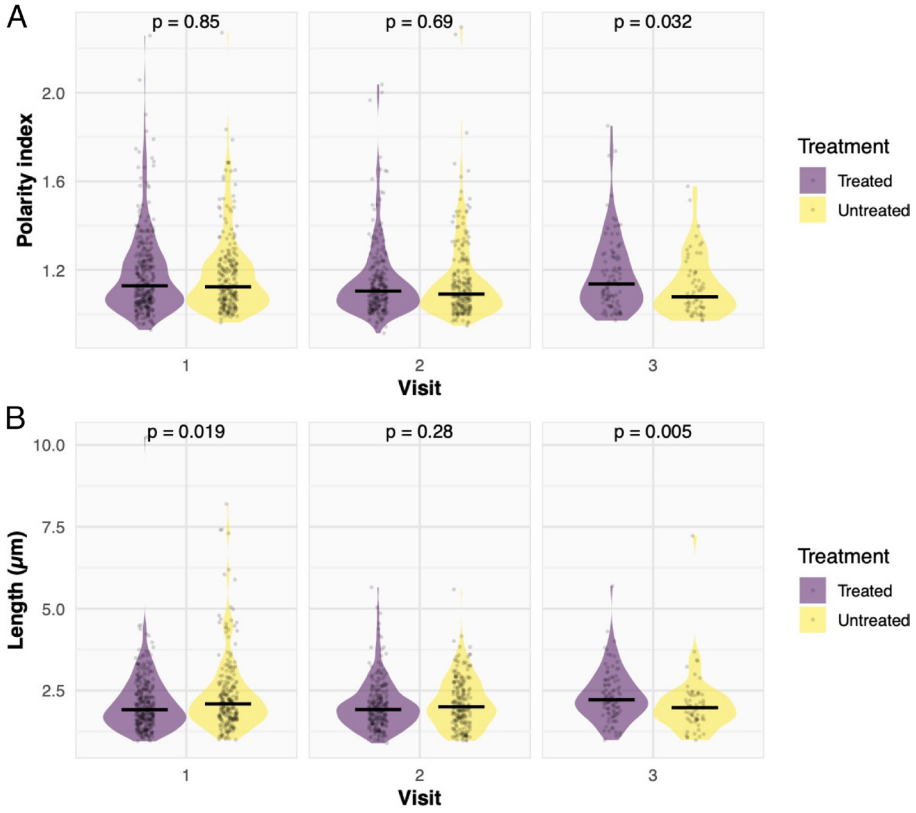

Fig. 7. Examining the change in DMN-trehalose phenotype and *Mtb* cell length through time. A comparison of (*A*) polarity index and (*B*) *Mtb* cell length between treatment groups at each visit. Polarity index is defined as the fluorescence intensity in arbitrary fluorescence units (AFU) of the brighter pole divided by the fluorescence intensity at the midcell. A Wilcoxon rank-sum test was performed.

induced sputum and BAL after EOT, the presence of which correlated with FDG-PET/CT findings and subsequent clinical outcomes (47).

An important complementary finding from our study was that the rate of clearance of aerosolized *Mtb* appeared to be unaffected by treatment (Fig. 5*B*). This conclusion was supported by the observation that treatment did not significantly impact the morphology of bacteria from the bioaerosol (Fig. 7). This is unlikely to be due to poor penetration of drugs since BAL sampling of patients on treatment demonstrate sterilizing concentrations of the standard TB drugs in PLF (48–51). Alternatively, this aerosolized *Mtb* population may exhibit phenotypic drug tolerance with clearance from this compartment primarily driven by innate immune processes. The ability of the aerosol phenotype of *Mtb* to persist in bioaerosols during and after TB therapy poses a previously under-recognized challenge to TB eradication within an individual. Furthermore, the isolation of viable *Mtb* from individuals not reaching a clinical threshold for TB diagnosis and treatment potentially expands the cohort of subclinical TB in the community—reinforcing very recent observations suggesting that subclinical disease might exist as long as 4 y prior to TB symptom onset (25). However, whether these organisms are transmissible to other hosts and have the capacity to revert to disease-causing phenotypes remains to be determined.

Table 4. Bioaerosol samples (n = 5) selected for *Mtb* whole-genome sequencing

Sample	Group	Visit	*Mtb* DNA copies	*Mtb* genome coverage (fold)	Lineage*
1	C	1	38,645	38.88	4.9
2	A	1	24,793	30.30	4.9
3	C	1	1,028	0.39	4.3
4	A	3	308	0.02	ND
5	C	4	89	0.06	ND

Parallel samples shown by group and visit number. All samples were from separate individuals. *Mtb* DNA copy number determined by ddPCR for the *Mtb*-specific RD9 target is shown after 50-d incubation in vitro. *Mtb* lineage was determined for three samples.
*ND, not determined.

It is also notable that symptom resolution is independent of treatment (Fig. 6*B*). The proportion of individuals both with detectable *Mtb* bacilli in sampled aerosol and the presence of TB symptoms decline over a similar timescale. This lends support to an immunological PLF clearance hypothesis in which *Mtb*-activated macrophages release tumor necrosis factor alpha and other cytokines which play a role in control of *Mtb* infection and at the same time generate systemic symptoms. These findings in the untreated participants (group C) may indicate transient and spontaneously resolving *Mtb* infection, analogous to the oscillating subgroup originally proposed decades ago (52) and reiterated recently (24). It remains uncertain, though, if this is due to a new TB exposure or to a perturbation of an existing, stable host–pathogen relationship. Sputum-Xpert Ultra-negative patients did present with clinical symptoms, but these resolved in parallel with decreasing *Mtb* numbers. DMN-trehalose uptake by bioaerosol-derived *Mtb* indicates that the captured bacilli are metabolically active but does not necessarily provide evidence that this specific phenotype has a role in TB transmission. However, unidentified *Mtb* transmitters, even at low levels, could account for a significant attributable proportion of community exposure exacerbated by long infectious periods and lack of debilitating disease, as highlighted by a recent modeling study (53).

Alternatively, the findings displaying in Figs. 5*B* and 6*B* may be interpreted as the presence of an intercurrent respiratory illness in the untreated group (group C) with subclinical *Mtb* colonization. Thus a self-limited course typical of common respiratory infections could explain the time-dependent resolution of symptoms. Furthermore the impact of intercurrent infection may potentiate *Mtb* release, with airway inflammation increasing aerosol generation, which would diminish on recovery. Such an interpretation could account for the parallel loss of symptoms and *Mtb* bioaerosol positivity via different mechanisms with a role for drug therapy in the clearance of the treated groups (groups A and B).

Limitations to this study include the pragmatic design (27) such that the patient groups were determined by the standard procedures and investigations of the South African TB Control Program (15). Therefore, the findings reflect a real-world healthcare scenario in South Africa and may lack the precision of a study with more thorough clinical characterization of patients—which might include sputum culture, as well as radiographical and immunological assays. In accordance with the preplanned pragmatic group allocation (27), no additional radiological investigations were carried out as part of this study and the exclusion of TB as likely diagnosis was made by TB clinicians without recourse to routine chest radiography. It is noteworthy, however, that only one individual initially allocated to sputum-Xpert Ultra-negative untreated group had ongoing symptoms which prompted a subsequent sputum Xpert Ultra-negative TB diagnosis and assignment to receive TB therapy. Additionally, the limited follow-up of 6 mo gave only a snapshot of the important longer-term relationship between the host and pathogen. It will be important to establish the role that continued *Mtb* infection may have for ongoing transmission, acquisition of new (super)infection, and progression to disease. This study was performed in one of the highest TB-burdened populations in the world, so the observations may not be generalizable to other lesser-burdened populations. In retrospect, sampling of healthy individuals from the community or indeed from a low TB prevalence setting would be optimal patient controls. However, at the time of planning the study extensive aerosol positivity was not anticipated in the untreated group (group C). Further studies should incorporate such individuals. It is also worth noting that the study was undertaken between June 2020 and June 2022, a period falling within the global Covid-19 pandemic with nationally mandated social interaction constraints and negative impacts on the health infrastructure including TB services.

Our knowledge of the TB host–pathogen relationship has been largely informed over the last 150 y by sputum-based studies. Our understanding of any disease is dependent on the assays and tools which are available to study it. New technologies such as FDG-PET/CT imaging are changing our perspective of within-host TB pathology (25), and developments in noninvasive bioaerosol sampling, such as modified facemasks (13) and our RASC sampling system, are revealing insights into the natural history of TB infection and disease. Applying these technologies longitudinally and to a wide spectrum of at-risk individuals can help to elucidate the complex interactions between the pathogen and the host throughout the human lifespan. This gives a window onto individual infectiousness with the potential to inform public health interventions, as well as provide an assay with potential utility for assessing targeted chemotherapy and as a metric in vaccine studies.

Materials and Methods

Study Design and Population. We recruited consecutive presumptive pulmonary TB patients over the age of 13 who self-presented to two community clinics serving two high-density, peri-urban residential areas south-west of Cape Town, South Africa. It should be noted that South Africa is a highly TB burdened country with an estimated incidence of 615 per 100,000 at the beginning of the study (54). Patients were identified by the presence of respiratory and/or constitutional symptoms on an initial triage screen. A subsequent clinical assessment, performed by clinic staff, either diagnosed TB (microbiologically or clinically) or did not. All patients triaged as presumptive TB on initial screening were recruited. This operationally pragmatic strategy was adopted to ensure broadly inclusive recruitment of individuals spanning the TB spectrum. A study protocol was published in advance (27) with the primary aim to compare proportions of *Mtb*-containing aerosols between TB patients who were sputum positive by the Xpert MTB/RIF Ultra (Xpert Ultra) assay (Cepheid, Sunnyvale, CA, USA) (group A) and sputum-Xpert Ultra–negative (group B). Assuming 20% bioaerosol positivity in group B, and 100% positivity in group A, a sample size of 250 was calculated to give 90% power to detect a difference between the groups (27). As an interim analysis showed no difference in the proportions of positive aerosols between groups A and B (2% 95% CI −11.1 to 22.7), the study was discontinued after recruitment of 102 patients on the grounds of futility. Ascertaining the prevalence proportion in group C was an exploratory aim and the isolation of a high bioaerosol-positive proportion in this group was unexpected. The detection of viable *Mtb* aerosols in the non-TB group, coupled with the concern that they might have unrecognized sputum-Xpert Ultra–negative TB disease, necessitated longitudinal monitoring and sampling equivalent to the treated TB patients. Sampling intervals of baseline, 2 wk, 2 mo, and 6 mo were therefore applied to all three groups, A–C. Notified TB patients (groups A and B) received standard short-course chemotherapy for 6 mo comprising 2 mo rifampicin, isoniazid, pyrazinamide, and ethambutol combination therapy, followed by 4 mo rifampicin plus isoniazid. Aerosol sampling at the initial visit was performed immediately before initiation of TB treatment in those diagnosed with TB.

Sampling Protocol and Data Collection. A direct sampling protocol was developed as previously described (27) and implemented with slight modifications (4). Briefly, participants were sequentially sampled at the Aerobiology Research Centre (ARC) using the RASC. The RASC is a HEPA-filtered enclosure designed for investigation of respiratory bioaerosol emissions from a single individual. The RASC accommodates a Tyvek-suited participant seated and sampled via a metallic elliptical cone which comfortably accommodates each participant's head (11). A unidirectional airflow is created by a high-flow (300L per minute) bespoke cyclone collector connected at the cone apex which extracts bioaerosol into sterile phosphate-buffered saline (PBS). Air enters the collector via a tangential nozzle which generates a liquid cyclone with particle inertia leading to deposition of bioaerosol from the airstream onto the wet wall. The exit airflow from the cone reaches a velocity of 12.5 m per second, enabling collection of expiratory aerosols. Seated participants were directed by a study nurse to complete a 15-min sampling protocol comprising 5-min sampling for each of 15 FVC maneuvers, tidal breathing, and 15 voluntary coughs. The bioaerosol samples were collected in three separate cones and assessed independently. Ozone sterilization and empty RASC sampling were performed between every participant to control for contamination. No *Mtb* bacilli were identified in these empty RASC controls. There was no contact between participants in the ARC, and they were required to wear N95 masks at all times when not inside the RASC. At each visit, questionnaires were completed to determine the presence of symptoms including persistent cough (>2 wk), recent weight loss, night sweats, loss of appetite, fever, hemoptysis, myalgias, and anosmia.

***Mtb* Detection Methods.** To confirm the specificity of *Mtb* detection, both DMN-trehalose and conventional *Mtb* identification methods were employed. Additional assays could not be sequentially applied post DMN-trehalose staining; moreover, the paucibacillary nature of the specimen precluded splitting of the sample. Therefore, for subsets of patient visits, additional bioaerosol sampling was performed in parallel to produce a second sample for investigation by Auramine O and/or Ziehl–Neelsen staining and/or DNA analysis using a ddPCR-based technique.

Sampling Processing. For each participant, bioaerosol material was captured in 5 to 10 mL PBS during each of the three respiratory maneuvers. After centrifugation at 3,000 × g for 10 min, the pellet was resuspended in 200 μL Middlebrook 7H9 medium and stained with the DMN-trehalose probe (29). Following overnight incubation in media containing DMN-trehalose, washed samples were added to a nanowell device (29). The devices were sealed with adhesive film and centrifuged

prior to visualization of the entire array by fluorescence microscopy. Detection and enumeration of fluorescent bacilli was based on DMN-trehalose incorporation and bacterial length and width assessments (20) by two separate microscopists for each sample, blinded to participants' samples and empty chamber control samples.

Auramine O and Ziehl–Neelsen Staining. A selection of parallel samples which were not subjected to DMN-trehalose staining were processed for Auramine O and/or Ziehl–Neelsen assays. After overnight incubation in 200 μL Middlebrook 7H9 medium, the aerosol pellet was smeared on a slide, and microscopy was performed using Auramine O fluorescent and/or Ziehl–Neelsen acid-fast staining in accordance with the MGIT procedure manual (55). *Mtb* H37Ra smears were prepared as positive controls for the staining techniques.

***Mtb* RD9 Detection and Quantification by ddPCR.** Extraction of *Mtb* genomic DNA was accomplished using a modified version of a previously published protocol (56) *Mtb* bioaerosol samples were incubated in 1:1 (v:v) Xpert buffer for 15 min, with vigorous shaking every 5 min. The buffer was neutralized by the addition of 1,200 μl of dH20, and the sample was centrifuged at 16,000 × g for 10 min. The supernatant was discarded, the pellet was resuspended in 20 μL Tris-EDTA (10 mM Tris and 1 mM EDTA, pH 8.0), and the sample was frozen at −70 °C for 10 min. After thawing at room temperature, the DNA was used for ddPCR. The primer/probe combinations and reaction conditions for *Mtb* RD9-specific ddPCR have been described previously (9). Serial dilutions of known concentrations of purified *Mtb* H37Rv genomic DNA were included as positive internal controls for ddPCR, and nuclease-free water was included as a negative control. Data generated from the ddPCR reactions were analyzed with the Umbrella pipeline (57) using only wells for which a minimum 10,000 droplets were detected.

***Mtb* Whole-Genome Sequencing.** Five samples with the highest number of RD9 copies following 50 d incubation of aerosol pellets (n = 64) in 200 μL Middlebrook 7H9-OADC medium at 37 °C were selected for WGS. Prior to library preparation, DNA that had been extracted as described above was purified using AMPure XP magnetic beads as described in ref. 58. Sequencing libraries were prepared using the Nextera XT kit and sequenced on an Illumina NovoSeq platform. WGS was analyzed according to previously described methods (59). Briefly, reads were trimmed using Trimmomatic v0.39 (60) with a sliding window of 5:20, and retaining reads with a minimum length of 20 was used to trim reads. Reads were then mapped to the reconstructed ancestor of the MTBC (61) using bwa v0.717 (62) Duplicates were removed using Picard v2.9.1 (63), prior to using Samtools v1.5 (64) and varScan v2.2.4 (65) call variants, with filters to exclude sites with fewer than 10 reads support and minimum base quality scores of 20. The resulting VCF files were used to search for lineage-defining SNPs as described (22). Only lineage-defining SNPs supported by at least 20 reads with an average Phred quality score of at least 30 are reported. Kraken2 (23) was implemented directly on Fastq files on the Sciensano Galaxy instance (66) with standard parameters against the full Kraken database.

Fluorescence Microscopy. Imaging was performed on a Zeiss Axio Observer 7 equipped with a 100× plan-apochromatic phase 3 oil immersion objective with a numerical aperture of 1.4. Epifluorescent illumination was provided by a 475 nm light-emitting diode (LED), and nonspecific fluorescence was removed with a Zeiss 38 HE filter set. Images were acquired using the Zeiss Zen software, and quantitative data were extracted using MicrobeJ (67).

Statistical Analyses. The bioaerosol positivity proportions of groups A, B, and C were compared using a Fisher's exact test and *Mtb* numbers with Wilcoxon rank-sum tests. Unadjusted odd ratios were used to investigate the impact of baseline demographic and clinical variables on the likelihood of baseline *Mtb* bacillary count positivity. Further logistical regression analyses assessed whether bioaerosol clearance was associated with baseline variables. The three separate time points (2 wk, 2 mo, and 6 mo) were investigated for clearance. For each analysis, data were dichotomized into count trajectories that cleared by that visit, defined as "no detectable DMN-trehalose *Mtb* bacilli", and those that did not clear. Additional analyses used the log-rank statistic for time to *Mtb* clearance and time to resolution of symptoms, defined as the first visit with no detectable DMN-trehalose *Mtb* bacilli and with no reported TB screening symptoms respectively. Clearance/resolution proportion for both outcomes were stratified by treatment (groups A and B vs. group C), previous history of TB disease, and HIV status. All statistical analyses were performed using R Core Team (2021) and the R software package, "survival".

Ethics Approval. This study was approved by the Human Research Ethics Committee (HREC/REF: 529/2019) of the University of Cape Town. Written informed consent, including for publication of medical details, was obtained from all participants, and assent was obtained from under 18-y-olds.

Data, Materials, and Software Availability. Data and code are available at https://github.com/benjaminpatterson1/ABC_study (68).

ACKNOWLEDGMENTS. R.W. discloses support for this work from the South African Medical Research Council [MRC-RFA-UFSP-01-2013/CCAMP] and the National Institute of Allergy and Infectious Diseases of the US NIH under award number R01AI147347 and through the Myco3V TB Research Unit (U19AI162584). D.F.W. acknowledges the support of the Strategic Health Innovations Partnerships Unit of the South African Medical Research Council with funds from the National Treasury under its Economic Competitiveness and Support Package and is grateful for funding from the Research Council of Norway (R&D Project 309592).

Author affiliations: [a]Amsterdam Institute for Global Health and Development, University of Amsterdam, Amsterdam 1105, The Netherlands; [b]South African Medical Research Council, National Health Laboratory Service, University of Cape Town Molecular Mycobacteriology Research Unit & Department of Science and Technology/National Research Foundation Centre of Excellence for Biomedical TB Research, Department of Pathology, Faculty of Health Sciences, University of Cape Town, Cape Town 7925, South Africa; [c]Institute of Infectious Disease and Molecular Medicine, Faculty of Health Sciences, University of Cape Town, Cape Town 7925, South Africa; [d]Aerobiology and TB Research Unit, Desmond Tutu Health Foundation, Cape Town 7975, South Africa; and [e]Wellcome Centre for Infectious Diseases Research in Africa, Faculty of Health Sciences, University of Cape Town, Cape Town 7925, South Africa

1. C. J. Roy, D. K. Milton, Airborne transmission of communicable infection–The elusive pathway. *N. Engl. J. Med.* **350**, 1710–1712 (2004), 10.1056/NEJMp048051.
2. S. B. Cohen *et al.*, Alveolar macrophages provide an early Mycobacterium tuberculosis niche and initiate dissemination. *Cell Host Microbe* **24**, 439–446.e4 (2018), 10.1016/j.chom.2018.08.001.
3. V. N. Houk, Spread of tuberculosis via recirculated air in a naval vessel: The Byrd study. *Ann. N. Y. Acad. Sci.* **353**, 10–24 (1980), 10.1111/j.1749-6632.1980.tb18901.x.
4. R. Dinkele *et al.*, Aerosolization of Mycobacterium tuberculosis by tidal breathing. *Am. J. Respir. Crit. Care Med.* **206**, 206–216 (2022), 10.1164/rccm.202110-2378OC.
5. J. Gebhart *et al.*, The human lung as aerosol particle generator. *J. Aerosol. Med.* **1**, 196–197 (1988).
6. G. R. Johnson *et al.*, Modality of human expired aerosol size distributions. *J. Aerosol Sci.* **42**, 839–851 (2011), 10.1016/j.jaerosci.2011.07.009.
7. J. A. Voynow, B. K. Rubin, Mucins, mucus, and sputum. *Chest* **135**, 505–512 (2009), 10.1378/chest.08-0412.
8. K. P. Fennelly, C. Acuna-Villaorduna, E. Jones-Lopez, W. G. Lindsley, D. K. Milton, Microbial aerosols: New diagnostic specimens for pulmonary infections. *Chest* **157**, 540–546 (2020), 10.1016/j.chest.2019.10.012.
9. B. Patterson *et al.*, Detection of Mycobacterium tuberculosis bacilli in bio-aerosols from untreated TB patients. *Gates Open Res.* **1**, 11 (2018).
10. B. Patterson, R. Wood, Is cough really necessary for TB transmission? *Tuberculosis* **117**, 31–35 (2019), 10.1016/j.tube.2019.05.003.
11. B. Patterson *et al.*, Sensitivity optimisation of tuberculosis bioaerosol sampling. *PLoS One* **15**, e0238193 (2020), 10.1371/journal.pone.0238193.
12. G. F. Theron *et al.*, Bacterial and host determinants of cough aerosol culture positivity in patients with drug-resistant versus drug-susceptible tuberculosis. *Nat. Med.* **26**, 1435–1443 (2020), 10.1038/s41591-020-0940-2.
13. C. M. Williams *et al.*, Exhaled Mycobacterium tuberculosis predicts incident infection in household contacts. *Clin. Infect. Dis.* **76**, e957–e964 (2023), 10.1093/cid/ciac455.
14. B. Patterson *et al.*, Cough-independent production of viable Mycobacterium tuberculosis in bioaerosol. *Tuberculosis* **126**, 102038 (2021), 10.1016/j.tube.2020.102038.
15. http://www.kznhealth.gov.za/family/NTCP_Adult_TB_Guidelines_2014.pdf (Accessed 5 April 2022).
16. T. C. Smith *et al.*, Morphological profiling of tubercule bacilli identifies drug pathways of action. *Proc. Natl. Acad. Sci. U.S.A.* **117**, 18744–18753 (2020), 10.1101/2020.03.11.987545.
17. T. J. de Wet, K. R. Winkler, M. Mhlanga, V. Mizrahi, D. F. Warner, Arrayed CRISPRi and quantitative imaging describe the morphotypic landscape of essential mycobacterial genes. *Elife* **9**, e60083 (2020), 10.7554/eLife.60083.
18. N. J. Garton *et al.*, Cytological and transcript analyses reveal fat and lazy persister-like bacilli in Tuberculous Sputum. *PLoS Med.* **5**, e75 (2008), 10.1371/journal.pmed.0050075.

19. S.-Y. Eum *et al.*, Neutrophils are the predominant infected phagocytic cells in the airways of patients with active pulmonary TB. *Chest* **137**, 122–128 (2010), 10.1378/chest.09-0903.
20. R. Dinkele *et al.*, Capture and visualization of live Mycobacterium tuberculosis bacilli from tuberculosis patient bioaerosols. *PLoS Pathog.* **17**, e1009262 (2021), 10.1371/journal.ppat.1009262.
21. F. P. Rodriguez-Rivera, X. Zhou, J. A. Theriot, C. R. Bertozzi, Acute modulation of mycobacterial cell envelope biogenesis by front-line tuberculosis drugs. *Angew. Chem. Int. Ed.* **57**, 5267–5272 (2018), 10.1002/anie.201712020.
22. F. Coll *et al.*, A robust SNP barcode for typing Mycobacterium tuberculosis complex strains. *Nat. Commun.* **5**, 4812 (2014), 10.1038/ncomms5812.
23. D. E. Wood, S. L. Salzberg, Kraken: Ultrafast metagenomic sequence classification using exact alignments. *Genome Biol.* **15**, R46 (2014), 10.1186/gb-2014-15-3-r46.
24. P. K. Drain *et al.*, Incipient and subclinical Tuberculosis: A clinical review of early stages and progression of infection. *Clin. Microbiol. Rev.* **31**, e00021-18 (2018), 10.1128/cmr.00021-18.
25. H. Esmail *et al.*, High resolution imaging and five-year tuberculosis contact outcomes. medRxiv [Preprint] (2023). https://doi.org/10.1101/2023.07.03.23292111 (Accessed 10 August 2023).
26. E. M. Lohmann *et al.*, Grading of a positive sputum smear and the risk of Mycobacterium tuberculosis transmission. *Int. J. Tuberc. Lung. Dis.* **16**, 1477–1484 (2012), 10.5588/ijtld.12.0129.
27. B. Patterson *et al.*, Bioaerosol sampling of patients with suspected pulmonary tuberculosis: A study protocol. *BMC Infect. Dis.* **20**, 587 (2020), 10.1186/s12879-020-05278-y.
28. J. T. Belisle *et al.*, Role of the major antigen of Mycobacterium tuberculosis in cell wall biogenesis. *Science* **276**, 1420–1422 (1997), 10.1126/science.276.5317.1420.
29. M. Kamariza *et al.*, Rapid detection of Mycobacterium tuberculosis in sputum with a solvatochromic trehalose probe. *Sci. Transl. Med.* **10**, eaam6310 (2018), 10.1126/scitranslmed.aam6310.
30. J. R. Glynn *et al.*, Whole genome sequencing shows a low proportion of tuberculosis disease is attributable to known close contacts in Rural Malawi. *PLoS One* **10**, e0132840 (2015), 10.1371/journal.pone.0132840.
31. L. M. Parsons *et al.*, Rapid and simple approach for identification of Mycobacterium tuberculosis complex isolates by PCR-Based genomic deletion analysis. *J. Clin. Microbiol.* **40**, 2339–2345 (2002).
32. A. L. den Hertog, S. Daher, M. Straetemans, M. Scholing, R. M. Anthony, No added value of performing Ziehl–Neelsen on auramine-positive samples for tuberculosis diagnostics. *Int. J. Tuberc. Lung. Dis.* **17**, 1094–1099 (2013), 10.5588/ijtld.12.0773.
33. C. Vilchèze, L. Kremer, Acid-fast positive and acid-fast negative Mycobacterium tuberculosis: The Koch paradox. *Microbiol. Spectr.* **5** (2017), 10.1128/microbiolspec.TBTB2-0003-2015.
34. P. Seiler *et al.*, Cell-wall alterations as an attribute of Mycobacterium tuberculosis in latent infection. *J. Infect. Dis.* **188**, 1326–1331 (2003), 10.1086/378563.
35. A. C. Brown *et al.*, Rapid whole-genome sequencing of Mycobacterium tuberculosis isolates directly from clinical samples. *J. Clin. Microbiol.* **53**, 2230–2237 (2015), 10.1128/JCM.00486-15.
36. N. Lozano *et al.*, Detection of minority variants and mixed infections in Mycobacterium tuberculosis by direct whole-genome sequencing on noncultured specimens using a specific-DNA capture strategy. *mSphere.* **6**, e0074421 (2021), 10.1128/mSphere.00744-21.
37. G. A. Goig *et al.*, Whole-genome sequencing of Mycobacterium tuberculosis directly from clinical samples for high-resolution genomic epidemiology and drug resistance surveillance: An observational study. *The Lancet Microbe* **1**, E175–E183 (2020b), 10.1016/s2666-5247(20)30060-4.
38. L. C. Malassez, W. Vignal, Tuberculose zoogloéique (Forme ou espéce de tuberculose sans bacilles). *Arch. Physiol. Norm. Patholog.* **2**, 369–412 (1883).
39. K. Takayama, L. Wang, H. L. David, Effect of isoniazid on the in vivo mycolic acid synthesis, cell growth, and viability of Mycobacterium tuberculosis. *Antimicrob. Agents Chemother.* **2**, 29–35 (1972).
40. K. Zainabadi *et al.*, An optimized method for purifying, detecting and quantifying Mycobacterium tuberculosis RNA from sputum for monitoring treatment response in TB patients. *Sci. Rep.* **12**, 17382 (2022), 10.1038/s41598-022-19985-w.
41. G. V. Mukamolova, O. Turapov, J. Malkin, G. Woltmann, M. R. Barer, Resuscitation-promoting factors reveal an occult population of Tubercle Bacilli in Sputum. *Am. J. Respir Crit. Care Med* **181**, 174–180 (2010b), 10.1164/rccm.200905-0661oc.
42. E. S. Chung, P. Kar, M. Kamkaew, A. Amir, B. B. Aldridge, Mycobacterium tuberculosis grows linearly at the single-cell level with larger variability than model organisms. bioRxiv [Preprint] (2023), https://doi.org/10.1101/2023.05.17.541183 (Accessed 10 August 2023).
43. J. de Gracia *et al.*, Diagnostic value of bronchoalveolar lavage in suspected pulmonary tuberculosis. *Chest* **93**, 329–332 (1988), 10.1378/chest.93.2.329.
44. M. Behr *et al.*, Transmission of Mycobacterium tuberculosis from patients smear-negative for acid-fast bacilli. *The Lancet* **353**, 444–449 (1999), 10.1016/s0140-6736(98)03406-0.
45. Y. L. Xie *et al.*, Transmission of Mycobacterium tuberculosis from patients who are nucleic acid amplification test negative. *Clin. Infect. Dis.* **67**, 1653–1659 (2018), 10.1093/cid/ciy365.
46. S. T. Malherbe *et al.*, Persisting positron emission tomography lesion activity and Mycobacterium tuberculosis mRNA after tuberculosis cure. *Nat. Med.* **10**, 1094–1100 (2016), 10.1038/nm.4177.
47. C. G. G. Beltran *et al.*, Investigating non-sterilizing cure in TB patients at the end of successful anti-TB therapy. *Front. Cell. Infect. Microbiol.* **10**, 443 (2020), 10.3389/fcimb.2020.00443.
48. J. K. O'Brien, M. E. Doerfler, T. J. Harkin, W. N. Rom, Isoniazid levels in the bronchoalveolar lavage fluid of patients with pulmonary tuberculosis. *Lung* **176**, 205–211 (1998), 10.1007/pl00007603.
49. J. E. Conte *et al.*, Effects of gender, AIDS, and acetylator status on intrapulmonary concentrations of isoniazid. *Antimicrob. Agents Chemother.* **46**, 3112–3112 (2002), 10.1128/aac.46.9.3112.2002.
50. E. Lopez-Varela *et al.*, Drug concentration at the site of disease in children with pulmonary tuberculosis. *J. Antimicrob. Chemother.* **77**, 1710–1719 (2022), 10.1093/jac/dkac103.
51. J. E. Conte, J. A. Golden, J. E. Kipps, E. T. Lin, E. Zurlinden, Effect of sex and AIDS status on the plasma and intrapulmonary pharmacokinetics of rifampicin. *Clin. Pharmacokinet.* **43**, 395–404 (2004), 10.2165/00003088-200443060-00003.
52. G. D. Gothi, Natural history of Tuberculosis, Wander-Tuberculosis Association of India Oration, Delivered on the occasion of the 32nd National Conference on TB and chest diseases held at Trivandrum, November 1977.
53. C. M. Issarow, N. Mulder, R. Wood, Environmental and social factors impacting on epidemic and endemic tuberculosis: A modelling analysis. *R. Soc. Open Sci.* **5**, 170726 (2018), 10.1098/rsos.170726.
54. World Health Organization, Global tuberculosis report, 2020. https://www.who.int/publications/i/item/97892400 (WHO, Geneva, Switzerland, 2020).
55. S. H. Siddiqi, S. Rüsch-Gerdes, MGIT procedure manual for bactec MGIT960 TB system (Foundation for Innovative New Diagnostics, Geneva, Switzerland, 2006).
56. A. K. Alame-Emane *et al.*, Use of genexpert remnants for drug resistance profiling and molecular epidemiology of Tuberculosis in Libreville. *Gabon. J. Clin. Microbiol.* **55**, 2105–2115 (2017), 10.1128/JCM.02257-16.
57. B. K. M. Jacobs *et al.*, Model-based classification for digital PCR: Your umbrella for rain. *Anal. Chem.* **89**, 4461–4467 (2017).
58. A. A. Votintseva *et al.*, Mycobacterial DNA extraction for whole-genome sequencing from early positive liquid (MGIT) cultures. *J. Clin. Microbiol.* **53**, 1137–1143, 10.1128/JCM.03073-14.
59. F. Menardo *et al.*, 2018) A tool to reduce large phylogenetic datasets with minimal loss of diversity. *BMC Bioinf.* **19**, 164 (2015), 10.1186/s12859-018-2164-8.
60. A. M. Bolger, M. Lohse, B. Usadel, Trimmomatic: A flexible trimmer for Illumina sequence data. *Bioinformatics* **30**, 2114–2120 (2014), 10.1093/bioinformatics/btu170.
61. I. Comas *et al.*, Human T cell epitopes of Mycobacterium tuberculosis are evolutionarily hyperconserved. *Nat. Genet.* **42**, 498–503 (2010), 10.1038/ng.590.
62. H. Li, R. Durbin, Fast and accurate long-read alignment with Burrows-Wheeler transform. *Bioinformatics.* **26**, 589–595 (2010), 10.1093/bioinformatics/btp698.
63. Broad Institute, "Picard tools" (Version 2.17.8, Broad Institute, 2018). GitHub repository. http://broadinstitute.github.io/picard/. Accessed 21 February 2018.
64. P. Danecek *et al.*, Twelve years of SAMtools and BCFtools. *Gigascience.* **10**, giab008 (2021), 10.1093/gigascience/giab008.
65. D. C. Koboldt *et al.*, VarScan 2: Somatic mutation and copy number alteration discovery in cancer by exome sequencing. *Genome Res.* **22**, 568–576 (2012), 10.1101/gr.129684.111.
66. B. Bogaerts *et al.*, A bioinformatics whole-genome sequencing workflow for clinical mycobacterium tuberculosis complex isolate analysis, validated using a reference collection extensively characterized with conventional methods and in silico approaches. *J. Clin. Microbiol.* **59**, e00202-21 (2021), 10.1128/JCM.00202-21.
67. A. Ducret, E. M. Quardokus, Y. V. Brun, MicrobeJ, a tool for high throughput bacterial cell detection and quantitative analysis. *Nat. Microbiol.* **1**, 16077 (2016), 10.1038/nmicrobiol.2016.77.
68. B. Patterson *et al.*, ABC_study GitHub repository. Github. https://github.com/benjaminpatterson1/ABC_study. Deposited 4 February 2024.